Towards an Auto-nowcasting System for Landslide Hazards

Cheng-Chien LIU[1, 2*], Hsiao-Yuan YIN[3], Hsiao-Wei CHUNG[2], Wei LUO[4] and Ke-Wei YAN[3]

[1] Dept. of Earth Sciences, National Cheng Kung University (Tainan, 70101 Taiwan)
[2] Global Earth Observation and Data Analysis Center, National Cheng Kung University (Tainan, 70101 Taiwan)
[3] Debris Flow Disaster Prevention Center, Soil and Water Conservation Bureau (Nantou, 54044 Taiwan)
[4] Dept. of Geography, Northern Illinois University (DeKalb, IL, USA)
*Corresponding author. E-mail: ccliu88@mail.ncku.edu.tw

This paper reports the efforts we made in the past four years to develop an auto-nowcasting system of landslide hazards, as well as the accuracy assessment of the I-Lan case in 2012 and 2013. This system uses a nondeterministic geometric mean model of landslide susceptibility index (*LSI*) to integrate three grid-based preparatory factors: slope, aspect, lithology, as well as one region-based factor: total flux. The weight of each preparatory factor is calculated by excluding the union of all shaded areas in the time series of satellite observations. The coefficients of the nondeterministic geometric mean model are determined by maximizing the positive right and negative right regions, and minimizing the missing and false alarm regions. By assuming that landslide hazard index (*LHI*) is related to *LSI* and accumulated precipitation (*AP*), the event-based inventory and *AP* for Typhoon Saola (11 July 2012) and Typhoon Soulik (12 July 2013) are used to develop and validate the *LHI* of I-Lan. Results show that the overall accuracy is as high as 85%. This *LHI* model has been implemented through SWCB Sediment-related Disaster Geospatial Information System (SDGIS) to provide an auto-nowcasting service with a map of five-level warning updated every hour.

Key words: preparatory factor, triggering factor, landslide susceptibility model, landslide hazard model, landslide inventory, nowcasting

1. INTRODUCTION

Landslide is one of the most common and dangerous natural hazards in mountainous regions, which alone caused a total death toll of at least 32,322 in 2,626 events between 2004 and 2010 [*Petley* 2012]. To minimize human and material losses, landslide-related maps are widely recognized to be crucial in implementing disaster prevention and mitigation strategies [*Hervas, et al.* 2003]. With the map of landslide susceptibility, for example, various measures can be implemented to build engineering structures and plan evacuation routes. Despite of the fact that different levels of assumptions and uncertainties are associated with different methods, the bottom line is to get a few hours of warning at least, in order to secure enough time of evacuation. This requires the nowcasting technique that provides a reliable prediction of the very near future from a large quantity of data series. This paper reports the efforts we made in the past four years to develop an auto-nowcasting system of landslide hazards, as well as the accuracy assessment of the I-Lan case.

2. METHOD

2.1 Shadow inventory and its influences on landslide susceptibility models

Landslide susceptibility describes the relative spatial likelihood for the occurrence of landslides, based on the landslide inventory prepared from space-borne or air-borne optical imagery. Most of the landslides are occurred in mountainous areas, where the imagery are acquired with some incline angles and the sun is not always in the nadir direction. Therefore, shadow is inevitable on these optical imageries. **Fig. 1** gives one example of mapping landslides triggered by the extreme rainfall of Typhoon Morakot in August of 2009. Most of the aftermath images available were acquired in the winter of 2009 or in the spring of 2010, because of the urgent needs to map the landslides and evaluate the damage. During that period of time, however, the sun elevation is low in the sub-tropical zone and the shadows could occupy as high as 30% of the entire image over the mountainous area, such as the example shown in **Fig. 1(b)**.

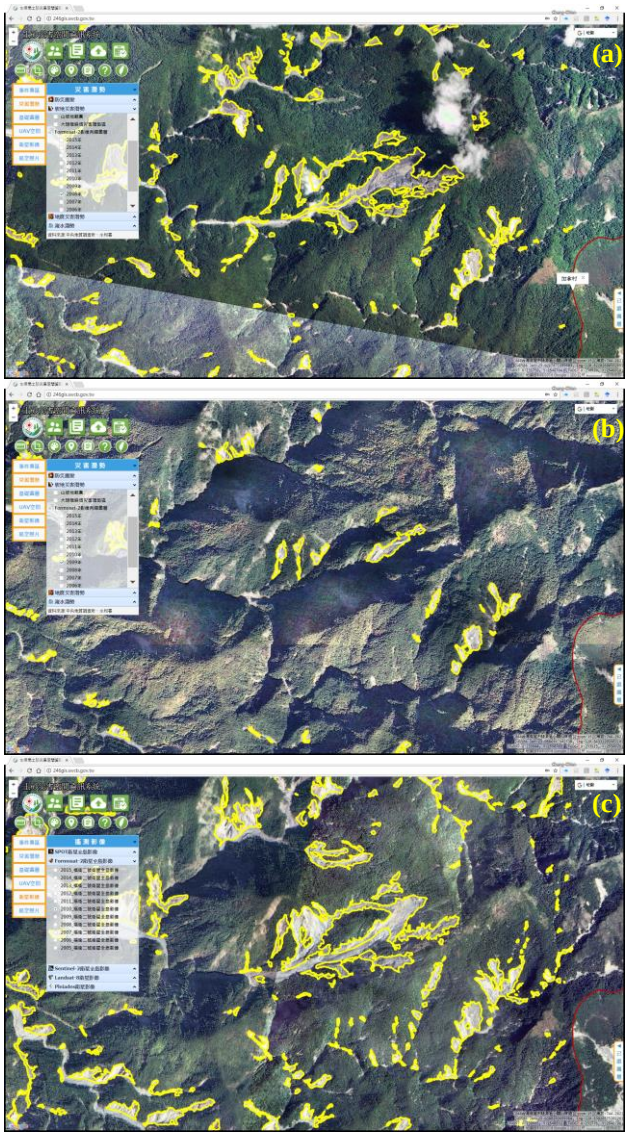

Fig. 1 Example of mapping landslides (yellow polygons) triggered by the extreme rainfall of Typhoon Morakot in August of 2009, using the Formosat-2 imagery acquired in (a) 2008, (b) 2009, and (c) 2010. A misleading conclusion of less landslide areas after Typhoon Morakot would be drawn, if the shadow inventory is not taken into account with special care.

The landslide areas delineated from the 2008 imagery (yellow polygons in **Fig. 1a**) are even larger than the landslide areas delineated from the 2009 imagery (yellow polygons in **Fig. 1b**). As a result, a misleading conclusion of less landslide areas after Typhoon Morakot would be drawn, if the shadow inventory is not taken into account with special care. The landslide areas delineated from the 2010 imagery (yellow polygons in **Fig. 1c**) clearly illustrates the destruction level of Typhoon Morakot: the landslide areas of 2010 are still much larger than the one of 2008, even after one year of recovery.

Two simple approaches were proposed and validated to compensate the error caused by shadows [*Lin, et al.* 2013], which requires a detailed shadow inventory prepared from the Expert Landslide and Shaded Area Delineation System [*Liu* 2015]. Our recent study evaluates the possible errors affecting landslide susceptibility models (LSMs) by neglecting the shadow inventory. We concluded that the weight of each preparatory factor *pf* should be calculated by excluding the union of all shaded areas in the time series of satellite observations.

2.2 A new region-based preparatory factor for landslide susceptibility models: the total flux

Current LSMs are mostly based on conditions represented by the data contained within each gridded cell, namely grid-based preparatory factor. Although drainage distance has been used to account for landslides occurring on slopes adjacent to main streams, *Liu et al.* [2016] demonstrated that drainage distance is not the best region-based preparatory factor, because the cells in the same drainage distance buffer zone may experience different total water flux as tributaries join the main stream when water flows downstream. Taking into account of the topography and hydrology conditions upstream of each gridded data cell, a new region-based preparatory factor total flux (TF) was proposed to represent the total flux of water in the stream. TF is proved to be strongly associated with the occurrence of landslides and is a good region-based preparatory factor for LSM [*Liu, et al.* 2016].

As suggested by *Liu et al.* [2004] that the preparatory factors should be obtainable and applicable anywhere, and reviewed by Süzen *et al.* [2011] that slope, aspect and lithology are the most influential natural factors, we build up a standard LSM that covers the entire country. Note that two cell-based factors, slope (**Fig. 2a**) and aspect (**Fig. 2b**), and the region-based factor, TF (**Fig. 2c**) are all derived from a digital elevation model (DEM) made available by the Ministry of Interior Affairs of Taiwan. The lithology map is provided by the Central Geological Survey of Taiwan at the scale of 1/250,000 (**Fig. 2d**). Detailed description of these preparatory factors can be referred to the project report [*GEODAC* 2014].

Note that only the mountainous regions of Taiwan are taken into consideration, which is about two-third of Taiwan. There are still some rooms of improvement of these preparatory factors. For example, the 5-m resolution DEM was produced before Typhoon Morakot in 2009, which might not be able to represent the current situation of surface elevation in some area. The lithology map provided at the scale of 1/250,000 is also too coarse comparing to the other data.

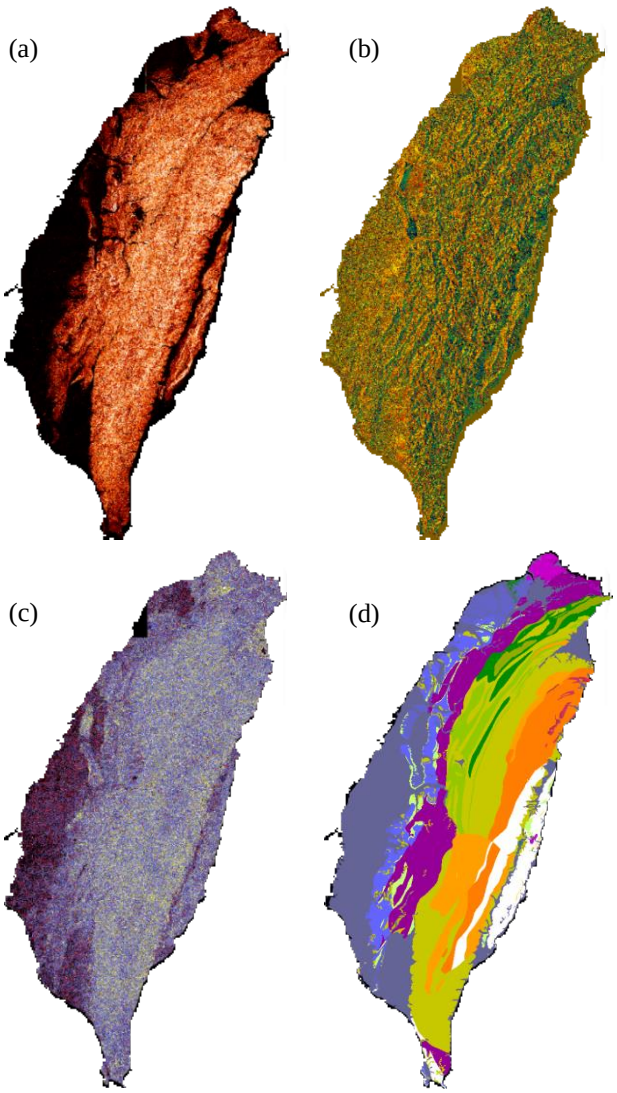

Fig. 2 Preparatory factor for landslide susceptibility models (a) slope, (b) aspect, (c) total flux, and (d) lithology.

2.3 Landslide susceptibility model based on geometric mean with indeterminate coefficients

LSM computes landslide susceptibility index (*LSI*) at each cell *j* of gridded raster data that indicates the susceptibility based on preparatory factors weighted according to importance. After excluding the union of all shaded areas in the time series of satellite observations and weighting each preparatory factor by the landslide inventory, two types of LSMs are usually employed, i.e., the arithmetic mean model [*Lee and Talib* 2005, *Yilmaz* 2009]

$$LSI(j) = \frac{1}{m}\sum_{k=1}^{m} W_{pf_k(i_k)} \qquad (1)$$

and the geometric mean model [*Fourniadis, et al.* 2007, *Nguyen and Liu* 2014]

$$LSI(j) = \left(\prod_{k=1}^{m} W_{pf_k(i_k)}\right)^{\frac{1}{m}} \qquad (2)$$

where *m* is the number of *pf* considered in *LSI*, *W* is the weight of *pf* at interval *i* defined as the frequency ratio [*Liu, et al.* 2016]. For one particular pf_k, i_k is the corresponding interval of pf_k at that cell *j*. *Liu et al.* [2004] discussed and recommended the geometric mean model (Eq. 2), which implies that the contribution of each *pf* is the same. This restriction can be removed by introducing a set of nondeterministic coefficients and searching an optimized value for each coefficient, namely the nondeterministic geometric mean model

$$LSI(j) = \prod_{k=1}^{m} W_{pf_k(i_k)}^{C_k} \qquad (3)$$

Note that Eq. (3) requires a well-defined criteria of optimization, which motivates us to revisit the evaluation indicators of landslide susceptibility model as described as follows.

2.4 Revisit the evaluation indicators of landslide susceptibility model

The percentage of landslide occurrence (POLO) and its cumulative (CPOLO) are commonly used as indicators to measure the performance of landslide susceptibility model. To evaluate the performance of landslide prediction or issue a warning, however, requires a fixed value of threshold that cannot be determined directly and solely from the CPOLO curve. Following the practice in weather forecast, two CPOLO curves are plotted within (yellow line) and outside (green line) the landslide areas, respectively, resulting in four regions of prediction: positive right, negative right, missing and false alarm (**Fig. 3**). Maximizing the first two (76.93%, 75.17%) and minimize the last two regions (23.07%, 24.83%) enables us to explicitly determine a new indicator that is especially suitable for determining the threshold: a value of 0.0125 for the case of I-Lan and the nondeterministic geometric mean model is

$$LSI = W_{\text{slope}}^{0.2746} \times W_{\text{aspect}}^{0.2712} \times W_{\text{TF}}^{0.2562} \times W_{\text{lithology}}^{0.2384} \qquad (4)$$

A detailed explanation of this new indicator, as well as Eq. (4) can be referred to the project report.

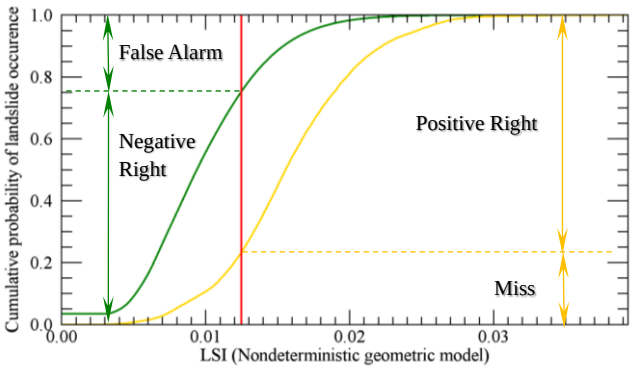

Fig. 3 Landslide susceptibility index of I-Lan calculated by using the nondeterministic geometric mean model (Eq. 3).

3. RESULTS

To attain the goal of nowcasting landslide hazards, the contribution of precipitation needs to be quantified first. Since the events of Typhoon and landslide are frequently reported in I-Lan, we prepare the event-based inventory and calculate the accumulated precipitation (*AP*) for Typhoon Saola (11 July 2012) and Typhoon Soulik (12 July 2013), respectively, as shown in **Fig. 4**.

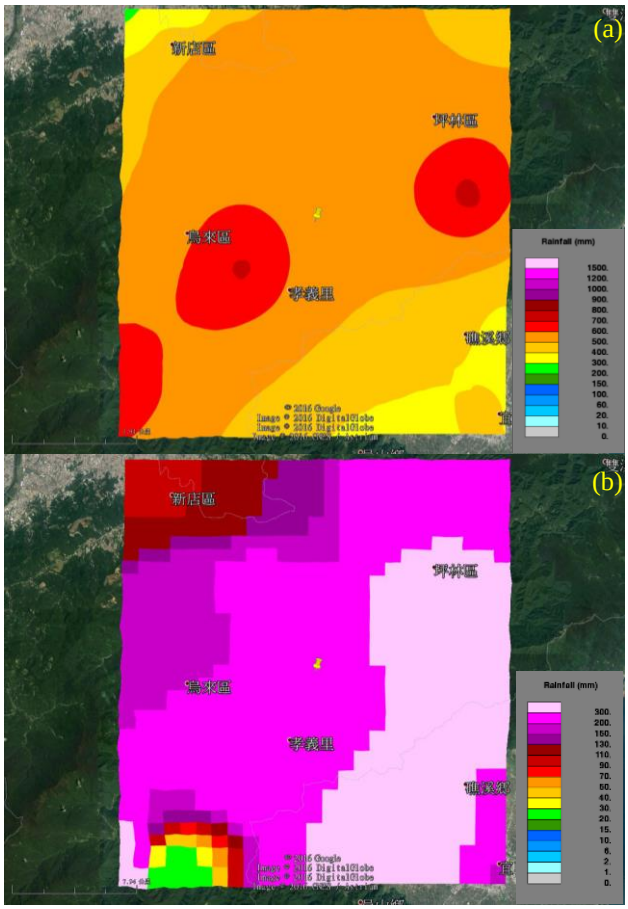

Fig. 4 Accumulated precipitation (*AP*) for (a) Typhoon Saola (11 July 2012), and (b) Typhoon Soulik (12 July 2013).

By assuming that landslide hazard index *LHI* is related to *LSI* and *AP* by

$$LHI = LSI \times AP^{C_{AP}} \qquad (5)$$

and employing the same technique of optimization using the event-based inventory of I-Lan of Typhoon Saola, a value of 0.0674 is obtained for C_{AP} (**Fig. 5a**). This *LHI* model is then validated by using the *AP* and event-based inventory of Typhoon Soulik (**Fig. 5b**). **Table 1** lists the accuracy in four regions of prediction: positive right, negative right, missing and false alarm. The overall accuracy is as high as 85%. By implementing this *LHI* model through SWCB Sediment-related Disaster Geospatial Information System (SDGIS) (http://246gis.swcb.gov.tw/) (**Fig. 6a**), we provide an auto-nowcasting service with a map of five-level warning updated every hour (**Fig. 6b**). Note this *LHI* model is only valid for I-Lan, since C_{AP} is a regional parameter that needs to be determined from the actual event.

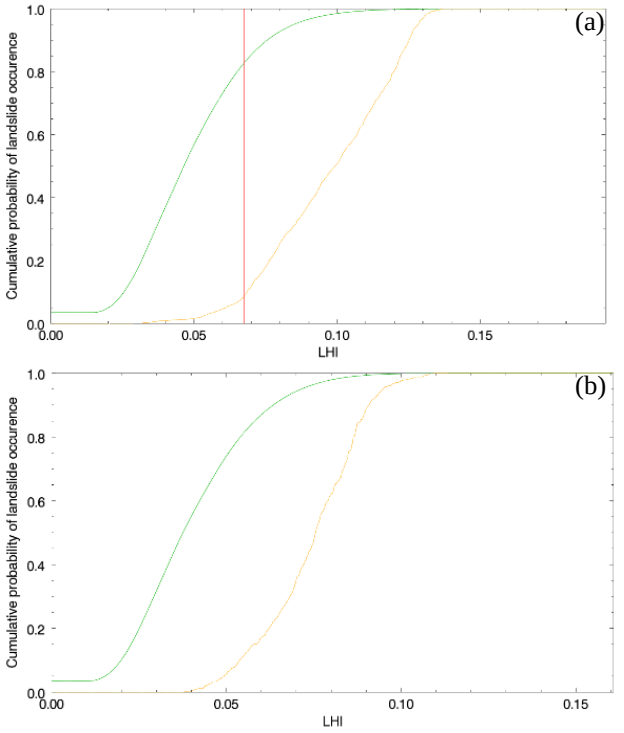

Fig. 5 (a) Development of *LHI* model using *AP* and the event-based inventory of I-Lan of Typhoon Saola (11 July 2012), and (b) Validation of *LHI* model using *AP* and the event-based inventory of I-Lan of Typhoon Soulik (12 July 2013).

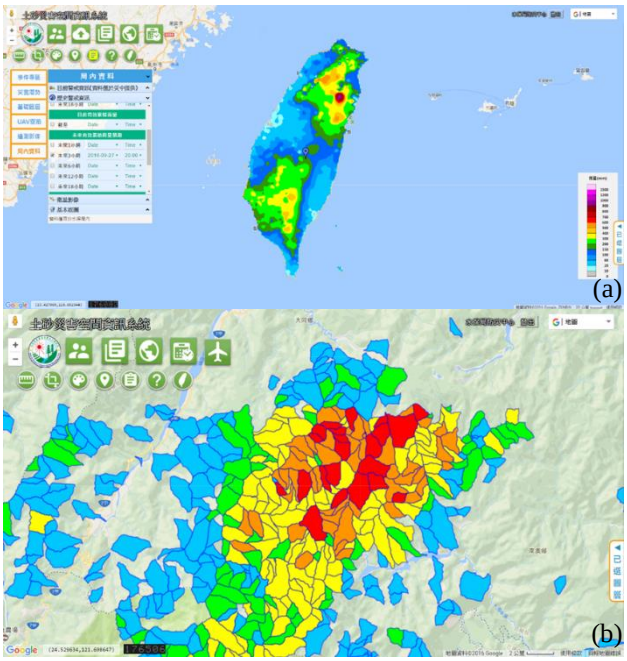

Fig. 6 (a) SWCB Sediment-related Disaster Geospatial Information System (SDGIS), and (b) an auto-nowcasting service with a map of five-level warning updated every hour.

Table 1 Accuracy report in four regions of prediction: positive right, negative right, missing and false alarm. (a) Development of *LHI* model using *AP* and the event-based inventory of I-Lan of Typhoon Saola (11 July 2012), and (b) Validation of *LHI* model using *AP* and the event-based inventory of I-Lan of Typhoon Soulik (12 July 2013).

	Development	Validation
LHI threshold	0.06744	0.0588
Positive Right (%)	91.62	84.73
Negative Right (%)	82.71	85.81
Miss (%)	8.38	15.27
False Alarm (%)	17.29	14.19

4. CONCLUDING REMARKS

An auto-nowcasting system of landslide hazards has been developed for Taiwan, which uses a nondeterministic geometric mean model of *LSI* to integrate three grid-based preparatory factors: slope, aspect, lithology, as well as one region-based factor: total flux. The weight of each preparatory factor is calculated by excluding the union of all shaded areas in the time series of satellite observations. The coefficients of the nondeterministic geometric mean model are determined by maximizing the positive right and negative right regions, and minimizing the missing and false alarm regions. By assuming that *LHI* is related to *LSI* and *AP*, the event-based inventory and *AP* for Typhoon Saola (11 July 2012) and Typhoon Soulik (12 July 2013) are used to develop and validate the *LHI* of I-Lan. Results show that the overall accuracy is as high as 85%. This *LHI* model has been implemented through SWCB Sediment-related Disaster Geospatial Information System (SDGIS) (http://246gis.swcb.gov.tw/) to provide an auto-nowcasting service with a map of five-level warning updated every hour.

ACKNOWLEDGMENT: This research is funded by Soil and Water Conservation Bureau, Council of Agriculture, Taiwan ROC, under Contract Nos. 106AS-7.3.1-SB-S2, as well as Ministry of Science and Technology of Taiwan ROC, under Contract Nos. MoST 106-2628-M-006-002.

REFERENCES

Fourniadis, I. G., J. G. Liu, and P. J. Mason (2007): Regional Assessment of Landslide Impact in the Three Gorges Area, China, Using Aster Data: Wushan-Zigui, Landslides, 4, pp. 267-278.

Global Earth Observation and Data Analysis Center (2014): 2014 Multi-Scale Remote Sensing Information System Data Establishment, Expansion and Maintenance, pp. 364. (in Chinese with English abstract)

Hervas, J., J. I. Barredo, P. L. Rosin, A. Pasuto, F. Mantovani, and S. Silvano (2003): Monitoring Landslides from Optical Remotely Sensed Imagery: The Case History of Tessina Landslide, Italy, Geomorphology, 54, pp. 63-75.

Lee, S., and J. Talib (2005): Probabilistic Landslide Susceptibility and Factor Effect Analysis, Environmental Geology, 47, pp. 982-990.

Lin, E.-J., C.-C. Liu, C.-H. Chang, I.-F. Cheng, and M.-H. Ko (2013): Using the Formosat-2 High Spatial and Temporal Resolution Multispectral Image for Analysis and Interpretation Landslide Disasters in Taiwan, Journal of Photogrammetry and Remote Sensing, 17, pp. 31-51.

Liu, C.-C. (2015): Preparing a Landslide and Shadow Inventory Map from High-Spatial-Resolution Imagery Facilitated by an Expert System, Journal of Applied Remote Sensing, 9, pp. 096080-096080.

Liu, C.-C., W. Luo, M.-C. Chen, Y.-T. Lin, and H.-L. Wen (2016): A New Region-Based Preparatory Factor for Landslide Susceptibility Models: The Total Flux, Landslides, 13, pp. 1049-1056.

Liu, J. G., P. J. Mason, N. Clerici, S. Chen, A. Davis, F. Miao, H. Deng, and L. Liang (2004): Landslide Hazard Assessment in the Three Gorges Area of the Yangtze River Using Aster Imagery: Zigui–Badong, Geomorphology, 61, pp. 171-187.

Nguyen, T.-T.-N., and C.-C. Liu (2014): Combining Bivariate and Multivariate Statistical Analyses to Assess Landslide Susceptibility in the Chen-Yu-Lan Watershed, Nantou, Taiwan, Sustainable Environment Research, 24, pp. 257-271.

Petley, D. (2012): Global Patterns of Loss of Life from Landslides, Geology, 40, pp. 927-930.

Süzen, M. L., and B. Ş. Kaya (2011): Evaluation of Environmental Parameters in Logistic Regression Models for Landslide Susceptibility Mapping, International Journal of Digital Earth, 5, pp. 338-355.

Yilmaz, I. (2009): Landslide Susceptibility Mapping Using Frequency Ratio, Logistic Regression, Artificial Neural Networks and Their Comparison: A Case Study from Kat Landslides (Tokat—Turkey), Computers & Geosciences, 35, pp. 1125-1138.